The air-broadened, near-infrared CO_2 line shape in the spectrally isolated regime: Evidence of simultaneous Dicke narrowing and speed dependence

David A. Long,[1] Katarzyna Bielska,[2] Daniel Lisak,[2] Daniel K. Havey,[3] Mitchio Okumura,[1] Charles E. Miller,[4] and Joseph T. Hodges[5,a)]

[1]*Division of Chemistry and Chemical Engineering, California Institute of Technology, Pasadena, California 91125, USA*
[2]*Instytut Fizyki, Uniwersytet Mikołaja Kopernika, ul. Grudziadzka 5/7, 87-100 Toruń, Poland*
[3]*Department of Chemistry and Biochemistry, James Madison University, Harrisonburg, Virginia 22807, USA*
[4]*Jet Propulsion Laboratory, California Institute of Technology, 4800 Oak Grove Drive, Pasadena, California 91109, USA*
[5]*Chemical and Biochemical Reference Data Division, National Institute of Standards and Technology, 100 Bureau Drive, Gaithersburg, Maryland 20899, USA*

(Received 1 July 2011; accepted 21 July 2011; published online 12 August 2011)

Frequency-stabilized cavity ring-down spectroscopy (FS-CRDS) was employed to measure air-broadened CO_2 line shape parameters for transitions near 1.6 μm over a pressure range of 6.7–33 kPa. The high sensitivity of FS-CRDS allowed for the first measurements in this wavelength range of air-broadened line shape parameters on samples with CO_2 mixing ratios near those of the atmosphere. The measured air-broadening parameters show several percent deviations (0.9%–2.7%) from values found in the HITRAN 2008 database. Spectra were fit with a variety of models including the Voigt, Galatry, Nelkin-Ghatak, and speed-dependent Nelkin-Ghatak line profiles. Clear evidence of line narrowing was observed, which if unaccounted for can lead to several percent biases. Furthermore, it was observed that only the speed-dependent Nelkin-Ghatak line profile was able to model the spectra to within the instrumental noise level because of the concurrent effects of collisional narrowing and speed dependence of collisional broadening and shifting. © *2011 American Institute of Physics*. [doi:10.1063/1.3624527]

I. INTRODUCTION

Recent carbon dioxide remote sensing missions have set unprecedented precision targets as demanding as 0.3% (change in atmospheric CO_2 mixing ratio of $\sim$1 μmol mol^{-1}).[1,2] These applications will require a detailed and thorough understanding of the near-infrared spectral line shapes of CO_2 and O_2 over the range of atmospherically relevant temperatures and pressures.[3] Of particular importance are higher order effects such as collisional narrowing, speed-dependent effects and line mixing which are yet to be incorporated into the vast majority of atmospheric retrievals which often employ the Voigt line profile. These effects will play an even greater role in next generation, active sensing missions[4–11] (including NASA's Active Sensing of CO_2 Emissions over Nights Days and Seasons, ASCENDS) where individual transitions in the near-infrared spectral region will be interrogated rather than entire bands, and where precise measurements of CO_2 concentrations will require exquisite knowledge of the spectral line shape.

While near-infrared CO_2 transitions have been extensively studied (for example, see Refs. 12–30 and the references found therein), non-Voigt line profiles have been employed only recently.[17–22,27,28,30] In a recent Fourier-transform spectroscopy (FTS) study, clear evidence of line narrowing was observed, and further it was found that using the Voigt profile (which does not include this effect) limited the uncertainty of the measured spectroscopic parameters to greater than $\sim$1%.[16] These findings led to a reanalysis of the FTS measurements using a speed-dependent Voigt profile with line mixing[17,18] which resulted in an $\sim$2% increase in the fitted broadening parameters and a small reduction in intensities (on average 0.22(56)%).

More recently Casa *et al*. used a laser absorption spectrometer to measure low-pressure (<5 kPa), self-broadened CO_2 line shapes near 5000 cm^{-1}.[27] Unlike previous FTS studies of CO_2 line shapes, they were able to clearly distinguish various line profiles because of the relatively high signal-to-noise ratio ($\sim$10 000:1) and spectral resolution ($\sim$1 MHz) of the measurements. However, they were unable to completely describe the observed line shapes with the Voigt, Galatry,[31] Nelkin-Ghatak,[32,33] speed-dependent Voigt,[34] correlated Galatry and Nelkin-Ghatak profiles (see Refs. 33 and 35). Notably, none of these theoretical profiles incorporated both collisional narrowing and speed-dependent effects. This lack of consistency between experiment and theory motivated the present work in which we apply frequency-stabilized cavity ring-down spectroscopy (FS-CRDS) to the measurement of near-infrared CO_2 line shapes. As previously demonstrated, the sensitivity and spectral fidelity of FS-CRDS make it an ideal technique for detailed study of subtle line shape effects.[36–43] Furthermore, the use of multi-spectrum fitting,[44–46] which simultaneously fits

a)Author to whom correspondence should be addressed. Electronic mail: joseph.hodges@nist.gov. Tel.: +1(301)975-2605. Fax: +1(301)869-5924.

spectra across a wide pressure range, can enable the collisional narrowing and speed-dependent effects to be separated and quantified. Below, we present FS-CRDS line shape measurements of an air-broadened near-infrared CO_2 transition near 6360 cm^{-1}, and we compare our measured Lorentzian broadening parameters to literature values. We also show that both collisional narrowing and speed-dependent effects need to be taken into account to best describe the observed pressure dependence of the line shape.

II. EXPERIMENT

Measurements were made using the frequency-stabilized cavity ring-down spectrometer located at the National Institute of Standards and Technology in Gaithersburg, Maryland.[47,48] This particular FS-CRDS instrument has been described earlier;[49] therefore, we will discuss only the most salient details herein.

FS-CRDS differs from traditional continuous wave (CW) CRDS in two fundamental ways. First, the intracavity distance is actively stabilized with respect to a reference laser. This length stabilization in turn stabilizes the entire comb of ring-down cavity transmission modes, thus providing an exceptionally linear, stable, and accurate spectrum frequency axis. In addition, FS-CRDS is a single-mode technique that enables the accurate measurement of sample absorption coefficient in terms of observed ring-down cavity decay time constants. FS-CRDS has been employed to measure ultra-weak transitions,[39,40] hyperfine structure[37] and rare isotopes,[42,43,49] and to produce reference standard spectroscopic data.[36,38,42,43,50]

For the measurements described herein the probe laser was an external cavity diode laser with an output power of ~15 mW and the reference laser was a frequency-stabilized HeNe laser with a long-term stability of 1 MHz (8 h). The ring-down mirrors had reflectivities of ~99.997% at the probe wavelength, corresponding to a finesse of ~105 000. Three hundred ring-down time constants were collected and averaged at each frequency step leading to a minimum detectable absorption coefficient of 3.5×10^{-11} cm^{-1} (see Fig. 1 of Ref. 49 for an Allan deviation plot with the given system parameters).

For the wavelength region investigated here, the sensitivity of FS-CRDS enables high signal-to-noise-ratio CO_2 absorption spectra to be acquired on air samples with CO_2 mixing ratios that are close to the current atmospheric background value (~390 μmol mol^{-1}). This capability of FS-CRDS is in contrast to similar near-infrared FTS measurements, which for reasons of sensitivity require CO_2 mixing ratios on the order of several percent (e.g., Ref. 15). In those cases self-broadening was not negligible by comparison to air broadening, whereas in the present study the small amount of CO_2 enabled direct measurement of CO_2 air-broadening parameters. In particular, the present measurements were made using NIST Standard Reference Material (SRM)® 1676, comprising carbon dioxide in air with a CO_2 mixing ratio of 367.81(37) μmol mol^{-1}. This dry gas sample contained nominally 20.8% oxygen and 0.98% argon with the remainder being nitrogen.

At pressures above 40.0 kPa (300 Torr) our spectra exhibited the effects of line mixing (line coupling). Specifically, we were no longer able to fit the spectra to within the instrumental noise level using any of the isolated line profile models described herein. Therefore, at pressures near or exceeding 40.0 kPa it was no longer possible to treat the transitions as being spectrally isolated. The present study aimed to examine CO_2 line shape behavior in the spectrally isolated pressure regime. Therefore, measurements were made over the pressure range 6.7–33 kPa (50–250 Torr) where no evidence of line mixing was observed. In a future study we will utilize these low pressure line shape results in combination with higher pressure (up to ~100 kPa) FS-CRDS measurements in order to quantify line mixing in air-broadened CO_2 spectra.

The sample pressure was measured using a NIST-calibrated diaphragm capacitance gauge having a full-scale response of 133.3 kPa (1000 Torr) and a relative standard uncertainty below 0.1%. All measurements were made at room temperature with no attempt made to control the cell temperature. The cell temperature was monitored using a NIST-calibrated 2.4 kΩ platinum thermistor. All measurements were made over the temperature range 297.7–299.4 K. The combined standard uncertainty in the cell temperature has recently been shown to be ~30 mK.[40] Measured air-broadening parameters were temperature corrected to $T_{ref} = 296$ K using the temperature dependences found in the HITRAN 2008 database.[51] As these measurements were made near the reference temperature, temperature corrections to the air-broadening parameters were small. Consequently, uncertainty in the temperature correction to the air-broadening parameter is negligible compared to the corresponding fit uncertainty.

III. SPECTRUM ANALYSIS

A. Line profiles

The measured spectra were fit with a variety of line profiles including the Voigt profile (VP), the Galatry profile (GP),[31] the Nelkin-Ghatak profile (NGP),[32,33] the speed-dependent Voigt profile (SDVP),[34] and the speed-dependent Nelkin-Ghatak profile (SDNGP).[33,52] The physical basis and mathematical form of these line profiles are described in Refs. 41 and 53; therefore, this will be discussed only briefly herein.

The VP is a convolution of Gaussian and Lorentzian line profiles and therefore accounts for Doppler and pressure broadening by treating these effects as statistically independent. The GP and NGP include the contribution of collisional (Dicke) narrowing,[54] which makes the observed Gaussian width narrower than the classical Doppler width. In the case of a relatively light perturber, the GP is more applicable than the NGP because the former uses a soft-collision model, whereas the latter uses a hard-collision model of velocity-changing collisions. The SDVP does not include collisional narrowing, but generalizes the VP by taking into account the dependence of collisional width and shift upon absorber speed. These effects usually cause line

narrowing and line asymmetry, respectively. Of the line profiles considered here, the SDNGP is the most general, because it includes both collisional narrowing and speed dependence.

B. Parameter definitions and the quadratic approximation

Detailed descriptions of all the theoretical line profiles used in the present analysis can be found in Refs. 41 and 53. However, to facilitate the interpretation of the experimental line shape parameters reported in this study we present formulas for calculating the SDNGP under the quadratic approximation of speed-dependence functions.[46,55,56] The absorption spectrum of an isolated transition $I(\nu - \nu_0)$ is the real part of the complex line profile denoted by $\tilde{I}(\nu - \nu_0)$, where ν is the optical frequency and ν_0 is the center frequency of the unperturbed line. In terms of dimensionless variables, the complex line shape function for the SDVP is

$$\tilde{I}_{\mathrm{SDVP}}(u) = \frac{2}{\pi^{3/2}} \int_{-\infty}^{\infty} dx e^{-x^2} \times x \left\{ \tan^{-1}[f(u,x)] + \frac{i}{2} \ln\left[1 + f(u,x)^2\right] \right\}, \tag{1}$$

where $u = (\nu - \nu_0)/\nu_D$ is the reduced spectral detuning. The variable of integration, $x = v/v_p$ is the reduced absorber speed, $v_p = \sqrt{2k_B T/m_A}$, m_A is the absorber mass, T is the gas temperature, and k_B is the Boltzmann constant. The Doppler width [full width at half maximum (FWHM)] is $\gamma_D = 2\sqrt{\ln(2)}\nu_D$, and the Lorentzian (collisional) width [half width at half maximum (HWHM)] and shift of line center are Γ and Δ, respectively. The function in the integrand of Eq. (1) is $f(u,x) = [u - dB_s(x) + x)]/[gB_w(x)]$, where $g = \Gamma/\nu_D$, $d = \Delta/\nu_D$, and $B_w(x)$ and $B_s(x)$ are the reduced speed-dependent collisional width and shift functions, respectively. Assuming a quadratic dependence for each of the speed-dependent collisional functions then

$$B_w(x) = 1 + a_w\left(x^2 - \frac{3}{2}\right), \qquad B_s(x) = 1 + a_s\left(x^2 - \frac{3}{2}\right) \tag{2}$$

define the broadening speed-dependence parameter a_w, and the shifting speed-dependence parameter a_s.[57] These two terms are treated as fitted parameters in the data analysis. At fixed temperature, a_w and a_s are expected to be independent of gas pressure.

The complex SDNGP line profile can be expressed in terms of the SDVP by

$$\tilde{I}_{\mathrm{SDNGP}}(u) = \frac{\tilde{I}_{\mathrm{SDVP}^*}(u)}{1 - \pi z \tilde{I}_{\mathrm{SDVP}^*}(u)}, \tag{3}$$

where $z = \nu_{nar}/\nu_D$ and $\tilde{I}_{\mathrm{SDVP}^*}(u)$ is the function $\tilde{I}_{\mathrm{SDVP}}(u)$ with $gB_w(x) + z$ substituted for $gB_w(x)$. Here, the narrowing frequency, ν_{nar}, accounts for the collisional narrowing effect, and at fixed temperature it is proportional to pressure. Thus, we define the collisional narrowing parameter as $\eta = \nu_{nar}/p$, which is a quantity that is also used in both the GP and the NGP.

IV. RESULTS AND DISCUSSION

In the present study, we measured transitions within the (30012) ← (00001) CO_2 band which is centered at wavelength $\lambda = 1576$ nm. We focused upon the $R16$ transition which is located at wave number $\tilde{\nu} = 6359.9673$ cm^{-1} and which has been proposed for use in NASA's ASCENDS active sensing mission.[5,11] The fitting of this transition included simultaneous fits to two much weaker transitions found within the wings of the main transition. These two weakly interfering transitions [(40012 ← 10001) $R18$ at 6359.8644 cm^{-1} and (31112 ← 01101) $R4$ at 6360.1130 cm^{-1}] have intensities which are only 0.3% and 1.7% of the main transition, respectively.[51] The top panel of Fig. 1 shows the measured absorption spectrum (symbols) and SDNGP fit (line) for the $R16$ transition, and the residuals obtained by individually

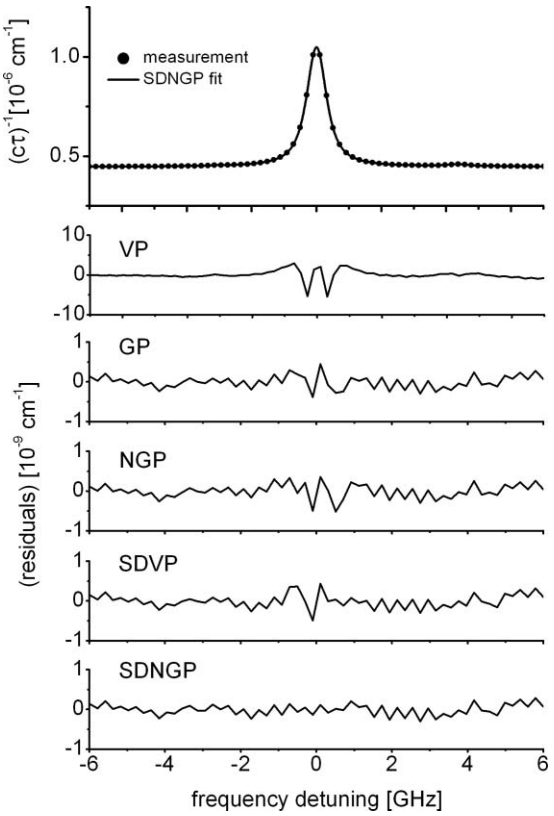

FIG. 1. Upper panel gives the measured FS-CRDS spectrum of the (30012) ← (00001) $R16$ transition of CO_2 and the single-spectrum SDNGP fit to these data. The sample gas was air with a CO_2 molar fraction of 367.81(37) μmol mol^{-1} at a total pressure of 13.3 kPa. Bottom panels are the corresponding fit residuals for the indicated line profiles. Fitting the VP to the measured spectrum leads to large, systematic residuals which are attributed to collisional narrowing and speed dependence. Note the tenfold difference in the vertical axis scale between the VP residual plot and those of the other cases. Use of the GP, NGP, and SDVP reduces the spectrum residuals approximately tenfold; however, only the SDNGP is able to model the spectrum to within the instrumental noise level. The spectrum signal-to-noise ratio (ratio of peak absorption to standard deviation of the fit residuals) for the SDNGP fit is ~5000:1.

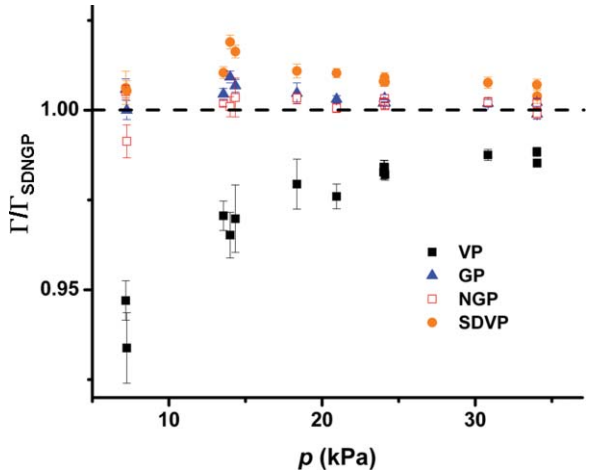

FIG. 2. Pressure dependence of the ratio of the air-broadened Lorentzian width, Γ, obtained by fitting various line profiles (VP, GP, NGP, SDVP) to that obtained with the SDNGP (denoted by Γ_{SDNGP}). These data correspond to the (30012) ← (00001) *R*16 transition of CO_2. Fitting spectra with the VP systematically underestimates the Lorentzian width and at a pressure of 7 kPa leads to a deviation of as much as 6%. Although the ratio $\Gamma_{VP}/\Gamma_{SDNGP}$ increases with pressure, it does not converge to unity even at $p = 40$ kPa. In contrast, $\Gamma_{NGP}/\Gamma_{SDNGP}$ is insensitive to pressure and has a mean value of 1.0014(9). The indicated error bars are given by the standard uncertainty from fitting each line profile and represent the dominant measurement uncertainty.

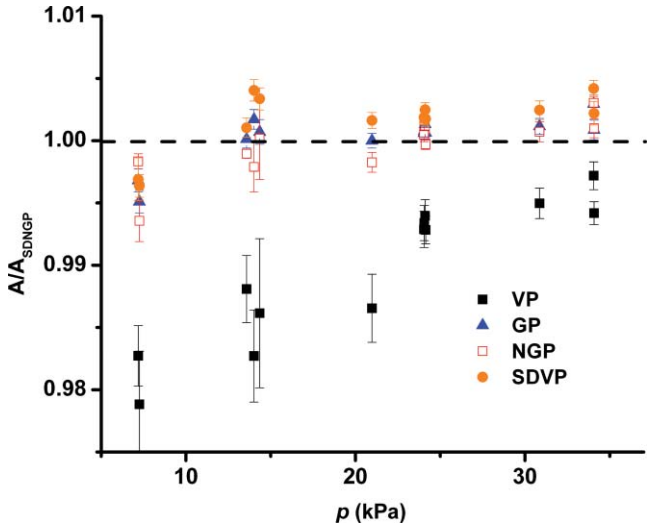

FIG. 3. Pressure dependence of the ratio of the spectrum area, *A*, obtained by fitting various line profiles (VP, GP, NGP, SDVP) to that obtained with the SDNGP (denoted by A_{SDNGP}). These data correspond to the air-broadened (30012) ← (00001) *R*16 transition of CO_2. Fitting spectra with the VP systematically underestimates the spectrum area, and at a pressure of 7 kPa use of the VP leads to a deviation of as much as 2% from the SDNGP value. The SDVP-fitted areas are on average about 0.15% greater than A_{SDNGP}, whereas the GP and NGP fitted areas are within 0.02% and 0.04%, respectively, of A_{SDNGP}. The indicated error bars are given by the standard uncertainty from fitting each line profile and represent the dominant measurement uncertainty. These ratios are not susceptible to uncertainty in CO_2 sample concentration.

fitting the VP, GP, SDVP, NGP, and SDNGP to the same measured spectrum are given in the bottom panels of this figure. Inspection of the VP residuals (note the unique *y*-axis scale for this residual panel) indicates that this profile underestimates the measured peak intensity and fails to capture the measured line shape. We attribute this lack of agreement to line narrowing. In contrast, the GP, NGP, and SDVP each models line narrowing (either collisional narrowing or speed dependence), and therefore fitting these profiles to the measured spectrum leads to vastly reduced residuals when compared to the VP. However, only the SDNGP, which includes both collisional narrowing and speed-dependent narrowing, models the spectrum to within the experimental noise level, resulting in a spectrum signal-to-noise ratio (ratio of peak absorption to standard deviation of fit residuals) of ~5000:1.

The choice of line profile utilized to model the measured spectra can have a considerable impact on the fitted spectroscopic parameters obtained at a given pressure. As can be seen in Figs. 2 and 3, fitting the VP to the measured spectra leads to significant deviations with respect to the measured Lorentzian width and spectrum area (proportional to line intensity). These deviations are especially large at low pressure (e.g., 6.7 kPa) where the Lorentzian width and spectrum area obtained through the fitting of the Voigt profile are smaller by as much as 6% and 2%, respectively, than those obtained with the SDNGP fits. In addition, we note that the Lorentzian width and line area parameters obtained from VP fits do not converge with those obtained using the other line profiles considered here, even at higher pressures. Furthermore, in the case of the VP, the fitted parameters have considerably larger uncertainties than those obtained with more advanced line profiles that are fit to the same data. Fitted parameters obtained with the GP, NGP, and SDVP are rather similar to those obtained with the SDNGP. Excluding the VP fits, we found that the maximum deviation in the fitted Lorentzian width and spectrum area were 1.9% and 0.6%, respectively.

Interestingly, for all the line profiles evaluated here the fitted Γ varies linearly with pressure, *p*, and as shown in Fig. 4 the slope, $d\Gamma/dp$, is similar for all cases. Note that $d\Gamma/dp$ corresponds to the air-broadening parameter, γ. However, with regard to the set of $\Gamma(p)$ obtained from VP fits, we find that there is an unphysical, negative-valued, *y*-intercept (y_0), which implies the occurrence of a nonlinear relationship for $\Gamma(p)$ at low pressure. We attribute this result to pressure-dependent line narrowing effects that are not modeled by the VP. This mode of analysis may have a profound impact upon laboratory and atmospheric determinations of γ. Specifically, when γ is evaluated as the ratio, Γ/p, where Γ is found by VP fits to a spectrum at a *single* pressure, then this measurement will tend to yield a broadening parameter which is lower than that obtained from other line profiles that incorporate narrowing effects. In the present case, the magnitude of this effect is nominally 2%. These findings were confirmed by computations in which Galatry line profiles were calculated across a range of pressures (using the collisional narrowing parameter calculated based upon the mass diffusion coefficient[58]) and then fit with Voigt line profiles. For the air-broadened CO_2 transition considered here, it is expected that the value of $d\Gamma/dp$ observed at pressures below 6.7 kPa would diverge from the higher pressure value.

As can be seen in Fig. 4, regardless of the line profile employed, the air-broadening parameters obtained from the present measurements show several-percent deviations from those found in the HITRAN 2008 database[51] (which

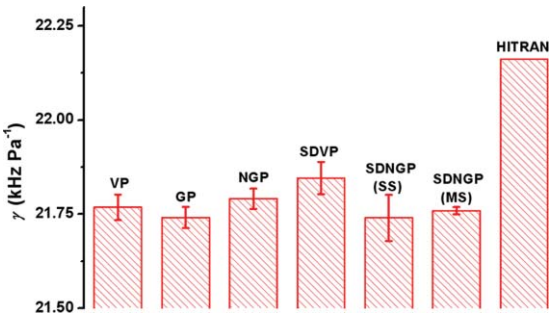

FIG. 4. Fitted air-broadening parameter, γ, at $T = 296$ K for the (30012) ← (00001) CO_2 $R16$ transition. The labels indicate the line profiles that were used, and SDNGP(SS) and SDNGP(MS) correspond to the single-spectrum fit and multi-spectrum fit cases, respectively, for the SDNGP. Except for the multi-spectrum fit case, these results were obtained by fitting the profiles to FS-CRDS spectra over the pressure range 6.7–34 kPa and then doing a weighted linear regression of $\Gamma(p) = \gamma p + y_0$ for each set of fitted Γ values. The air-broadening parameter for the SDNGP(MS) case is 21.758(9) kHz Pa^{-1}. Note that each of the fitted values is ~2% lower than the HITRAN 2008 value, which is equal to 22.16 kHz Pa^{-1}.[51] The factor 1 cm^{-1} atm^{-1} ≡ 295.872 kHz Pa^{-1} can be used to convert these values into the conventional units for γ (cm^{-1} atm^{-1}). The error bars are given by the uncertainty in γ derived from the linear regression and represent the dominant measurement uncertainty.

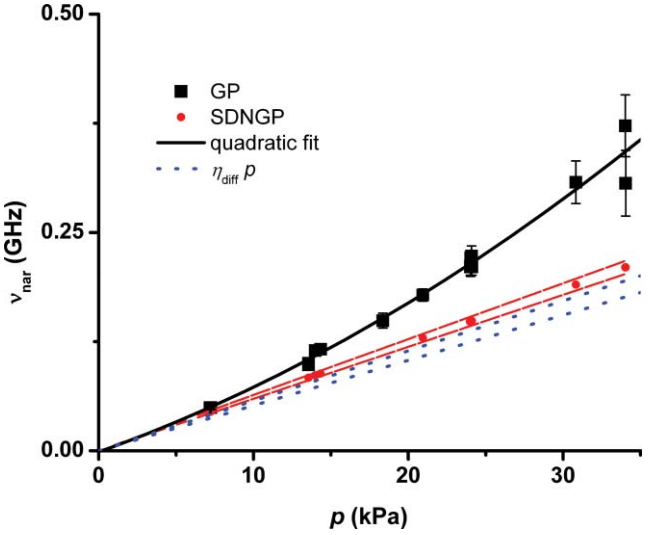

FIG. 5. Collisional narrowing frequency, ν_{nar}, as a function of pressure for the air-broadened (30012) ← (00001) $R16$ CO_2 transition. For single-spectrum fits of the GP (square symbols) the ν_{nar} values have an unphysical, quadratic pressure dependence caused by concurrent collisional (Dicke) narrowing and speed-dependent narrowing. The indicated narrowing frequencies (red circles) are obtained when the same spectra are simultaneously fit over the entire pressure range with the SDNGP. This multi-spectrum analysis uses the SDNGP subject to the constraint that $\nu_{nar} = \eta_{SDNGP} \times p$. Importantly, the fitted collisional narrowing parameter (the slope of the line formed by the red circles, shown with its standard uncertainty in dashed red lines), agrees well with the diffusion-based value, η_{diff} (Ref. 58). We find that η_{SDNGP} = 6.18(21) kHz Pa^{-1} and η_{diff} = 5.44(27) kHz Pa^{-1}. The indicated error bars are given by the standard uncertainty in the fitted narrowing frequency and represent the dominant measurement uncertainty.

are based upon Ref. 16 which were supplemented with the results of Ref. 30). Note that these deviations greatly exceed the precision requirement (0.3%) of present remote sensing missions.[1,2] The HITRAN 2008 air-broadening parameters in this band are based upon FTS measurements of CO_2-air mixtures with several percent CO_2.[18] As the self-broadening parameters of CO_2 are generally ~40% larger than the air-broadening parameters,[51] these results were extrapolated to natural abundance of CO_2. We speculate that either this extrapolation or other line shape effects (e.g., line mixing) are the source of this deviation. Note that the SDNGP-retrieved, air-broadening parameter for the $R16$ transition is 21.758(9) kHz Pa^{-1} (0.07354(3) cm^{-1} atm^{-1}) at T = 296 K. We observed similar deviations from the HITRAN 2008 air-broadening parameters for the $R14$, $R18$, $P16$, and $P18$ transitions of CO_2; each of which was lower than the HITRAN 2008 parameters by 0.9%–2.7%. It is worth noting that our value for the $R16$ transition agrees with that of Toth *et al.*[15] (0.0733(3) cm^{-1} atm^{-1}), but significantly differs from those of Devi *et al.* [18] (0.07471(8) cm^{-1} atm^{-1}), Predoi-Cross *et al.*[20] (0.07517(6) cm^{-1} atm^{-1}), and Li *et al.*[59] (0.07106(8) cm^{-1} atm^{-1}).

The pressure dependence of the narrowing frequency obtained by fitting the GP to our measured spectra is shown in Fig. 5. If collisional narrowing were the only source of line narrowing, we would expect the narrowing parameter to exhibit a linear dependence on pressure. However, in the present case, we observe a quadratic dependence on pressure. Similar behavior is observed for NGP fits. This nonlinearity indicates the simultaneous occurrence of collisional (Dicke) narrowing and speed-dependent narrowing (e.g., Refs. 41 and 60–63).

The SDNGP accounts for both of these narrowing effects and is therefore an appropriate line profile within this pressure regime (<35 kPa). However, since both collisional narrowing and speed dependence narrow the total line width, their fitted values can become correlated. In order to remove this correlation, the two mechanisms of narrowing can be separated based on their different pressure dependencies. Specifically, the collisional narrowing frequency is given by $\nu_{nar} = \eta p$ in which η is the collisional narrowing parameter, whereas the quadratic approximation speed-dependent parameters a_w and a_s are independent of pressure.[64] Thus, we have utilized multi-spectrum fitting[44,45] to simultaneously fit spectra across a given range of pressures. This multi-spectrum fitting procedure produces a single value for each of the narrowing and asymmetry parameters (i.e., η, a_w, and a_s). With this approach, the SDNGP profiles were simultaneously fit to 13 spectra spanning the pressure range 7–34 kPa, yielding fitted values for these three parameters. We note that the respective baselines were constrained to those obtained from the individual fits. Four representative measured spectra, their fitted profiles, and their respective sets of fit residuals are shown Fig. 6. From the complete multi-spectrum fit of the SDNGP, we find η = 6.18(21) kHz Pa^{-1}, a_w = 0.042(8), and a_s = 0.08(2). Note that the spectrum signal-to-noise ratio ranges from 2150 to 3600 and is not as high as that obtained with the SDNGP single-spectrum fit shown in Fig. 1. This reduction in fit quality is caused by linearly constraining the pressure-dependence of the line shape parameters, such that the fit precision is limited by imprecision in the temperature and pressure measurements over the duration of the multi-spectrum data.

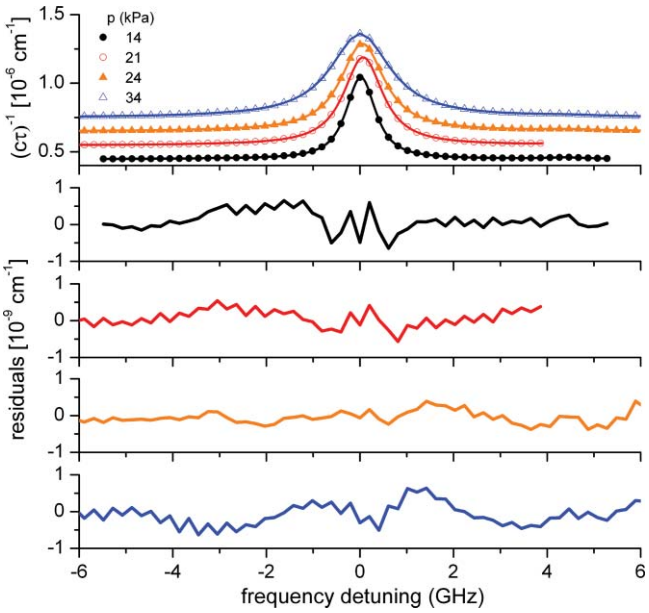

FIG. 6. Four representative measured and modeled absorption spectra of air-broadened (30012) ← (00001) *R*16 CO_2 transition. The top panel shows measured spectra (symbols) and multi-spectrum SDNGP fit (lines). For clarity, the three highest-pressure spectra are successively offset in the vertical direction in increments of 10^{-7} cm^{-1}. The bottom four panels (increasing pressure from top to bottom) give the residuals of the SDNGP global fit (measured spectrum—fitted profile) for each pressure. Prior to implementing the multi-spectrum fit, each individual spectrum is corrected for a baseline etalon.

When all velocity changing collisions contribute to the line narrowing, the collisional narrowing parameter can be calculated based on the mass diffusion coefficient of the absorber, D, and pressure and temperature, as $\eta_{\text{diff}} = k_B T/(2\pi m_a D p)$. For dilute mixtures of CO_2 in air we estimate that $\eta_{\text{diff}} = 5.44(27)$ kHz Pa^{-1} (0.0184(9) cm^{-1} atm^{-1}),[58] and as can be seen in Fig. 5, the collisional narrowing parameter, η_{SDNGP} which was obtained from the multi-spectrum fit agrees well (relative difference of <15%) with η_{diff}. This agreement supports use of the SDNGP for modeling the collisional narrowing effect[61] in the present case and is consistent with the underlying assumption (required also for the GP and NGP) that all velocity changing collisions fully contribute to the line narrowing. Therefore, it appears unlikely that models accounting for correlations between velocity- and phase-changing collisions such as the CNGP (Ref. 33) or the CS-DNGP (Ref. 65) are required to describe our measured CO_2 line shapes in this pressure range.

Casa *et al.*[27] recently observed that fitting the GP to self-broadened CO_2 spectra (near $\lambda = 2.0$ μm) over the range $p = 0.7$–4.0 kPa led to collisional narrowing parameters that exceeded η_{diff} by roughly a factor of two. This discrepancy between measured and calculated narrowing parameters can be explained by the simultaneous occurrence of collisional narrowing and speed-dependent effects, as found in the present study. We anticipate that a multi-spectrum fit of the SDNGP to their measured spectra, equivalent to that presented here, would yield a physically consistent collisional narrowing parameter that is either equal to or less than η_{diff}.

V. CONCLUSIONS

Air-broadened near-infrared CO_2 transitions were measured with frequency-stabilized cavity ring-down spectroscopy at CO_2/air mixing ratios close to those in the atmosphere. We focused upon the *R*16 transition of the (30012) ← (00001) band (located near 6360 cm^{-1}) which has been proposed for use in NASA's ASCENDS active sensing mission.[5,11] We reported the first measurements of the air-broadening parameters of this transition at near-atmospheric mixing ratios. We find that our measured broadening parameters differ by up to several percent (0.9%–2.7%) relative to those in the HITRAN 2008 database.

The measured spectra showed unambiguous evidence of collisional narrowing. Failure to account for this line narrowing (i.e., through the application of the commonly used Voigt line profile) led to biases of several percent in the measured broadening parameters and intensities and to relatively large uncertainties by comparison to those obtained with more complex line profiles. In addition, it was found that both collisional narrowing and speed dependence of collisional broadening and shifting played a significant role in this pressure range (6.7–33 kPa). Of the line profiles considered here, the SDNGP (which includes both of these effects) was the only one that modeled individual spectra to within the instrumental noise level. Finally, excellent agreement was observed between the fitted and mass diffusion-based narrowing parameters when SDNGPs were simultaneously fit to spectra acquired over a range of pressure. This result indicated that the use of correlation line profile models such as the correlated-NGP or correlated-SDNGP is likely unnecessary in the present case. For the pressure range considered, we found no evidence of line mixing, although in general, we expect that more comprehensive models which include line mixing effects will be required to accurately predict the evolution of CO_2 absorption spectra for pressures exceeding ~40 kPa.

ACKNOWLEDGMENTS

David A. Long was supported by the National Science Foundation and National Defense Science and Engineering Graduate Fellowships. Daniel K. Havey was supported by a National Research Council postdoctoral fellowship at the National Institute of Technology (NIST), Gaithersburg, MD, and Katarzyna Bielska and Daniel Lisak were supported by the Polish MNISW Project No. N N202 1255 35. Part of the research described in this paper was performed at the Jet Propulsion Laboratory, California Institute of Technology, under contract with the National Aeronautics and Space Administration (NASA). Additional support was provided by the Orbiting Carbon Observatory (OCO) project, a NASA Earth System Science Pathfinder (ESSP) mission; the NASA Upper Atmospheric Research Program grants NNG06GD88G and NNX09AE21G; the NASA Atmospheric Carbon Observations from Space (ACOS) grant 104127-04.02.02; and the NIST Greenhouse Gas Measurements and Climate Research Program.

[1]D. Crisp, R. M. Atlas, F. M. Breon, L. R. Brown, J. P. Burrows, P. Ciais, B. J. Connor, S. C. Doney, I. Y. Fung, D. J. Jacob, C. E. Miller, D. O'Brien, S. Pawson, J. T. Randerson, P. Rayner, R. J. Salawitch, S. P. Sander, B. Sen, G. L. Stephens, P. P. Tans, G. C. Toon, P. O. Wennberg, S. C. Wofsy, Y. L. Yung, Z. Kuang, B. Chudasama, G. Sprague, B. Weiss, R. Pollock, D. Kenyon, and S. Schroll, in *Trace Constituents in the Troposphere and Lower Stratosphere* (Pergamon-Elsevier Science Ltd., Kidlington, 2004), vol. 34.

[2]C. E. Miller, D. Crisp, P. L. DeCola, S. C. Olsen, J. T. Randerson, A. M. Michalak, A. Alkhaled, P. Rayner, D. J. Jacob, P. Suntharalingam, D. B. A. Jones, A. S. Denning, M. E. Nicholls, S. C. Doney, S. Pawson, H. Boesch, B. J. Connor, I. Y. Fung, D. O'Brien, R. J. Salawitch, S. P. Sander, B. Sen, P. Tans, G. C. Toon, P. O. Wennberg, S. C. Wofsy, Y. L. Yung, and R. M. Law, J. Geophys. Res., [Atmos.] **112**(D10), D10314, doi:10.1029/2006JD007659 (2007).

[3]C. E. Miller, L. R. Brown, R. A. Toth, D. C. Benner, and V. M. Devi, C. R. Phys. **6**(8), 876 (2005).

[4]G. Ehret, C. Kiemle, M. Wirth, A. Amediek, A. Fix, and S. Houweling, Appl. Phys. B **90**(3–4), 593 (2008).

[5]J. B. Abshire, H. Riris, G. R. Allan, C. J. Weaver, J. P. Mao, X. L. Sun, W. E. Hasselbrack, S. R. Kawa, and S. Biraud, Tellus B **62**(5), 770 (2010).

[6]R. T. Menzies and D. M. Tratt, Appl. Opt. **42**(33), 6569 (2003).

[7]F. Gibert, P. H. Flamant, J. Cuesta, and D. Bruneau, J. Atmos. Ocean. Technol. **25**(9), 1477 (2008).

[8]F. Gibert, L. Joly, I. Xueref-Remy, M. Schmidt, A. Royer, P. H. Flamant, M. Ramonet, B. Parvitte, G. Durry, and V. Zeninari, Spectroc. Acta A **71**(5), 1914 (2009).

[9]G. D. Spiers, R. T. Menzies, J. Jacob, L. E. Christensen, M. W. Phillips, Y. H. Choi, and E. V. Browell, Appl. Opt. **50**(14), 2098 (2011).

[10]S. R. Kawa, J. Mao, J. B. Abshire, G. J. Collatz, X. Sun, and C. J. Weaver, Tellus B **62**(5), 759 (2010).

[11]K. Numata, J. R. Chen, S. T. Wu, J. B. Abshire, and M. A. Krainak, Appl. Opt. **50**(7), 1047 (2011).

[12]C. E. Miller and L. R. Brown, J. Mol. Spectrosc. **228**(2), 329 (2004).

[13]R. A. Toth, L. R. Brown, C. E. Miller, V. M. Devi, and D. C. Benner, J. Mol. Spectrosc. **239**(2), 221 (2006).

[14]R. A. Toth, L. R. Brown, C. E. Miller, V. M. Devi, and D. C. Benner, J. Mol. Spectrosc. **239**(2), 243 (2006).

[15]R. A. Toth, C. E. Miller, V. M. Devi, D. C. Benner, and L. R. Brown, J. Mol. Spectrosc. **246**(2), 133 (2007).

[16]R. A. Toth, L. R. Brown, C. E. Miller, V. M. Devi, and D. C. Benner, J. Quant. Spectrosc. Radiat. Transf. **109**(6), 906 (2008).

[17]V. M. Devi, D. C. Benner, L. R. Brown, C. E. Miller, and R. A. Toth, J. Mol. Spectrosc. **245**(1), 52 (2007).

[18]V. M. Devi, D. C. Benner, L. R. Brown, C. E. Miller, and R. A. Toth, J. Mol. Spectrosc. **242**(2), 90 (2007).

[19]A. Predoi-Cross, A. Unni, W. Liu, I. Schofield, C. Holladay, A. R. W. McKellar, and D. Hurtmans, J. Mol. Spectrosc. **245**(1), 34 (2007).

[20]A. Predoi-Cross, W. Liu, C. Holladay, A. V. Unni, I. Schofield, A. R. W. McKellar, and D. Hurtmans, J. Mol. Spectrosc. **246**(1), 98 (2007).

[21]T. Hikida, K. M. T. Yamada, M. Fukabori, T. Aoki, and T. Watanabe, J. Mol. Spectrosc. **232**(2), 202 (2005).

[22]T. Hikida and K. M. T. Yamada, J. Mol. Spectrosc. **239**(2), 154 (2006).

[23]I. Pouchet, V. Zeninari, B. Parvitte, and G. Durry, J. Quant. Spectrosc. Radiat. Transf. **83**(3–4), 619 (2004).

[24]S. Nakamichi, Y. Kawaguchi, H. Fukuda, S. Enami, S. Hashimoto, M. Kawasaki, T. Umekawa, I. Morino, H. Suto, and G. Inoue, Phys. Chem. Chem. Phys. **8**(3), 364 (2006).

[25]B. V. Perevalov, A. Campargue, B. Gao, S. Kassi, S. A. Tashkun, and V. I. Perevalov, J. Mol. Spectrosc. **252**(2), 190 (2008).

[26]B. V. Perevalov, S. Kassi, V. I. Perevalov, S. A. Tashkun, and A. Campargue, J. Mol. Spectrosc. **252**(2), 143 (2008).

[27]G. Casa, R. Wehr, A. Castrillo, E. Fasci, and L. Gianfrani, J. Chem. Phys. **130**(18), 184306 (2009).

[28]L. Joly, F. Gibert, B. Grouiez, A. Grossel, B. Parvitte, G. Durry, and V. Zeninari, J. Quant. Spectrosc. Radiat. Transf. **109**(3), 426 (2008).

[29]Z. Majcherova, P. Macko, D. Romanini, V. I. Perevalov, S. A. Tashkun, J. L. Teffo, and A. Campargue, J. Mol. Spectrosc. **230**(1), 1 (2005).

[30]A. Predoi-Cross, A. R. W. McKellar, D. C. Benner, V. M. Devi, R. R. Gamache, C. E. Miller, R. A. Toth, and L. R. Brown, Can. J. Phys. **87**(5), 517 (2009).

[31]L. Galatry, Phys. Rev. **122**(4), 1218 (1961).

[32]M. Nelkin and A. Ghatak, Phys. Rev. **135**(1A), A4 (1964).

[33]S. G. Rautian and I. I. Sobelman, Sov. Phys. Usp. **9**(5), 701 (1967).

[34]P. R. Berman, J. Quant. Spectrosc. Radiat. Transf. **12**(9), 1331 (1972).

[35]P. L. Varghese and R. K. Hanson, Appl. Opt. **23**(14), 2376 (1984).

[36]D. J. Robichaud, J. T. Hodges, L. R. Brown, D. Lisak, P. Maslowski, L. Y. Yeung, M. Okumura, and C. E. Miller, J. Mol. Spectrosc. **248**(1), 1 (2008).

[37]D. A. Long, D. K. Havey, M. Okumura, C. E. Miller, and J. T. Hodges, Phys. Rev. A **81**(6), 064502 (2010).

[38]D. A. Long, D. K. Havey, M. Okumura, C. E. Miller, and J. T. Hodges, J. Quant. Spectrosc. Radiat. Transf. **111**(14), 2021 (2010).

[39]D. A. Long, D. K. Havey, M. Okumura, H. M. Pickett, C. E. Miller, and J. T. Hodges, Phys. Rev. A **80**, 042513 (2009).

[40]D. K. Havey, D. A. Long, M. Okumura, C. E. Miller, and J. T. Hodges, Chem. Phys. Lett. **483**(1–3), 49 (2009).

[41]D. Lisak, J. T. Hodges, and R. Ciurylo, Phys. Rev. A **73**(1), 012507 (2006).

[42]D. J. Robichaud, L. Y. Yeung, D. A. Long, M. Okumura, D. K. Havey, J. T. Hodges, C. E. Miller, and L. R. Brown, J. Phys. Chem. A **113**, 13089 (2009).

[43]D. A. Long, D. K. Havey, S. S. Yu, M. Okumura, C. E. Miller, and J. T. Hodges, J. Quant. Spectrosc. Radiat. Transf. (in press).

[44]D. Lisak, P. Maslowski, A. Cygan, K. Bielska, S. Wojtewicz, M. Piwinski, J. T. Hodges, R. S. Trawinski, and R. Ciurylo, Phys. Rev. A **81**(4), 042504 (2010).

[45]D. C. Benner, C. P. Rinsland, V. M. Devi, M. A. H. Smith, and D. Atkins, J. Quant. Spectrosc. Radiat. Transf. **53**(6), 705 (1995).

[46]D. Lisak, D. K. Havey, and J. T. Hodges, Phys. Rev. A **79**(5), 052507 (2009).

[47]J. T. Hodges, H. P. Layer, W. W. Miller, and G. E. Scace, Rev. Sci. Instrum. **75**(4), 849 (2004).

[48]J. T. Hodges and R. Ciurylo, Rev. Sci. Instrum. **76**(2), 023112 (2005).

[49]D. A. Long, M. Okumura, C. E. Miller, and J. T. Hodges, Appl. Phys. B (in press).

[50]D. J. Robichaud, J. T. Hodges, P. Maslowski, L. Y. Yeung, M. Okumura, C. E. Miller, and L. R. Brown, J. Mol. Spectrosc. **251**(1–2), 27 (2008).

[51]L. S. Rothman, I. E. Gordon, A. Barbe, D. C. Benner, P. F. Bernath, M. Birk, V. Boudon, L. R. Brown, A. Campargue, J. P. Champion, K. Chance, L. H. Coudert, V. Dana, V. M. Devi, S. Fally, J. M. Flaud, R. R. Gamache, A. Goldman, D. Jacquemart, I. Kleiner, N. Lacome, W. J. Lafferty, J. Y. Mandin, S. T. Massie, S. N. Mikhailenko, C. E. Miller, N. Moazzen-Ahmadi, O. V. Naumenko, A. V. Nikitin, J. Orphal, V. I. Perevalov, A. Perrin, A. Predoi-Cross, C. P. Rinsland, M. Rotger, M. Simecková, M. A. H. Smith, K. Sung, S. A. Tashkun, J. Tennyson, R. A. Toth, A. C. Vandaele, and J. Vander Auwera, J. Quant. Spectrosc. Radiat. Transf. **110**(9–10), 533 (2009).

[52]B. Lance, G. Blanquet, J. Walrand, and J. P. Bouanich, J. Mol. Spectrosc. **185**(2), 262 (1997).

[53]J. M. Hartmann, C. Boulet, and D. Robert, *Collisional Effects on Molecular Spectra* (Elsevier, Amsterdam, 2008).

[54]R. H. Dicke, Phys. Rev. **89**(2), 472 (1953).

[55]D. Priem, F. Rohart, J. M. Colmont, G. Wlodarczak, and J. P. Bouanich, J. Mol. Struct. **517**, 435 (2000).

[56]R. Ciurylo, Phys. Rev. A **58**(2), 1029 (1998).

[57]J. Ward, J. Cooper, and E. W. Smith, J. Quant. Spectrosc. Radiat. Transf. **14**(7), 555 (1974).

[58]W. J. Massman, Atmos. Environ. **32**(6), 1111 (1998).

[59]J. S. Li, K. Liu, W. J. Zhang, W. D. Chen, and X. M. Gao, J. Mol. Spectrosc. **252**(1), 9 (2008).

[60]D. Lisak, G. Rusciano, and A. Sasso, J. Mol. Spectrosc. **227**(2), 162 (2004).

[61]P. Duggan, P. M. Sinclair, A. D. May, and J. R. Drummond, Phys. Rev. A **51**(1), 218 (1995).

[62]J. F. D'Eu, B. Lemoine, and F. Rohart, J. Mol. Spectrosc. **212**(1), 96 (2002).

[63]D. Lisak, G. Rusciano, and A. Sasso, Phys. Rev. A **72**(1), 012503 (2005).

[64]P. Duggan, P. M. Sinclair, R. Berman, A. D. May, and J. R. Drummond, J. Mol. Spectrosc. **186**(1), 90 (1997).

[65]D. Robert, J. M. Thuet, J. Bonamy, and S. Temkin, Phys. Rev. A **47**(2), R771 (1993).